Check for updates

MnO$_2$/Carbon Composites for Supercapacitor: Synthesis and Electrochemical Performance

Dan Wu[1], Xiubo Xie[1], Yuping Zhang[1], Dongmei Zhang[2], Wei Du[1]*, Xiaoyu Zhang[1]* and Bing Wang[3]

[1] School of Environment and Material Engineering, Yantai University, Yantai, China, [2] Shandong Institute for Food and Drug Control, Jinan, China, [3] CAS Key Laboratory for Biomedical Effects of Nanomaterials and Nanosafety, Institute of High Energy Physics, Chinese Academy of Sciences, Beijing, China

As an emerging energy storage device, the supercapacitor with high energy density, fast charging/discharging, and good cycle stability has aroused great interest. The performance of supercapacitors mainly depend on the electrode material. Manganese dioxide (MnO$_2$) has emerged as one of the most promising electrode materials for high theoretical specific capacitance, wide potential range, high electrochemical activity, and environmental friendliness. However, its deteriorated volume expansion and inherently low conductivity limit its development and application in supercapacitors. To circumvent the mentioned issues, the porous, thin film, or layered composite materials were prepared to enhance the electrical conductivity and specific surface area of MnO$_2$. Carbon materials are the ideal choice to compound with MnO$_2$ owing to their low electrical resistance, significant thermal stability, large specific surface area, and porosity. Up to now, several kinds of MnO$_2$/carbon composites as supercapacitor electrodes have been designed and fabricated. Herein, we give a concise review of the latest researches on MnO$_2$/carbon supercapacitor electrodes, focusing on the fabrication strategies and analyzing the influencing factors of electrochemical performance of MnO$_2$/carbon materials. An outlook on the possible development directions in future of designing high-performance MnO$_2$/carbon materials for the current challenges is also provided.

Keywords: MnO$_2$, carbon materials, composites, electrode material, supercapacitor
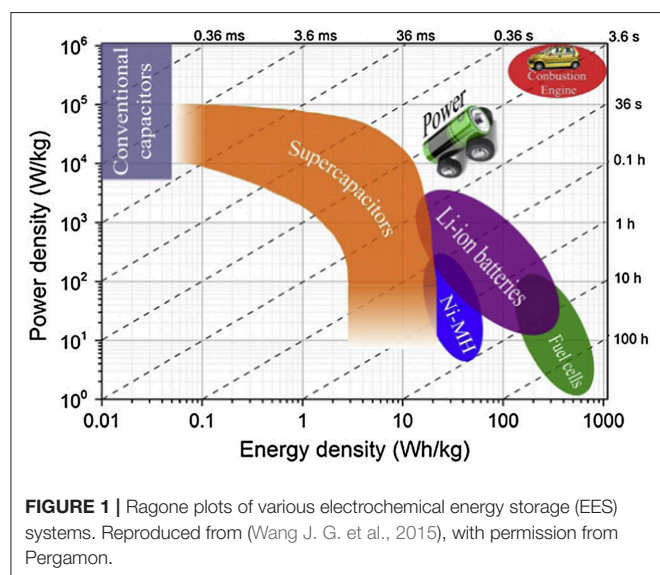
INTRODUCTION

Nowadays, with the excessive consumption of traditional energy sources such as coal, oil, and natural gas, the increasingly severe global climate and deteriorating ecological environment have caused a global crisis that endangers human survival. The development and utilization of eco-friendly renewable energy become an extremely imminent task all over the world. In the past decade, solar, hydro, wind, and tidal energy and other renewable energy sources have greatly alleviated serious problems in the energy and environmental fields (Yang et al., 2011; Xie X. et al., 2019). However, abundant and clean renewable energy mentioned above cannot be widely applied directly owing to the limitation of natural conditions and the poor tunability and stability of generating electricity. Therefore, reliable electrochemical energy storage (EES), including fuel cells, ion batteries, and supercapacitors, is extremely necessary to achieve efficient storage, conversion, and further utilization of the above energy sources (Palchoudhury et al., 2019). The Ragone plots

in **Figure 1** shows the relationship between power density and energy density for several typical EES systems (Wang J. G. et al., 2015). Among them, electrochemical capacitors, which are also known as supercapacitors, are considered to be a new generation of green energy storage device (Díaz-Delgado and Doherty, 2016), with greater capacitance than conventional capacitors and higher output power and longer life than lithium-ion batteries (Zhang Q. Z. et al., 2018). Combined with its simple structure, high power density, fast charging, and pollution-free effects in the production process, supercapacitors are widely applied in portable electronics, data backup, hybrid electric vehicle, aerospace, and other fields (Salinas-Torres et al., 2019).

According to the charge storage mechanism, supercapacitors are generally classified as electrochemical double-layer capacitors (EDLCs) and pseudocapacitors (Wang G. P. et al., 2012). Energy storage and conversion of EDLCs are accomplished by static charge separation in the Helmholtz layer. Common active materials with double-layer electrodes are mostly carbon materials, which can rapidly complete the charging and discharging process and remain stable, but their capacitance and energy density are relatively low (<10 Wh kg^{-1}) (Liang and Xin, 2015). The storage capacity of pseudocapacitors, compared with EDLCs, can be greatly improved owing to a series of reversible redox reactions on the surface/bulk phase of the electrode material (Conway, 1999). Transition metal oxides (Tajik et al., 2017) and conductive polymers (Snook et al., 2011) are commonly used as electrode materials for pseudocapacitors. The performance of supercapacitors is primarily dependent on the activity and kinetics of the electrode material. Therefore, it is very important to select suitable electrode materials, further optimize their structure, and improve their activity and kinetics to enhance the electrochemical properties of supercapacitors (Trudeau, 2013). Carbon materials and manganese dioxide (MnO$_2$), as the most representative materials of EDLCs and pseudocapacitors, respectively, show their unique advantages in energy storage.

Carbon is one of the most closely and important elements for humans in nature and plays an important role in our existing ecosystems (Candelaria et al., 2012). It has various electronic orbital properties of sp, sp^2, and sp^3 hybridization, and the anisotropy of sp^2 leads to various orientations of crystals and other arrays (Yu et al., 2018). Therefore, different kinds of carbon materials are formed by different chemical bonds. In particular, functional carbon materials considered to be ideal electrode materials for supercapacitors have attracted great attention owing to their low resistance, good electrical conductivity, high porosity, and large specific surface area (He et al., 2013; Borenstein et al., 2017). The EDLCs composed of carbon material form stable electric double layers by attracting mutually opposite charges at the electrode/electrolyte interface, which can achieve energy store through the physical electrostatic adsorption/desorption of charges. The energy storage mechanism is conducive to increasing the conductivity of the electrode to improve the specific capacity and energy density. Moreover, the carbon material can transform the structure and bonding mode of the composite material, thereby improving charging/discharging rate capability and cycle stability. For pure carbon materials, their specific capacitance and energy density ($100 \sim 300$ F g^{-1}, $5 \sim 7$ Wh kg^{-1}) largely depends on specific surface area, porosity, and pore size distribution (Wang et al., 2019b). In recent years, a large number of functional carbon nanomaterials with related excellent properties, such as activated carbon (AC) (Faraji and Ani, 2015), graphene [including graphene oxide (GO) and reduced GO (rGO)] (Shi et al., 2018), carbon nanotubes (CNTs) (Qian et al., 2012), carbon nanofibers (CNFs) (Peng et al., 2016), and carbon aerogel (CA) (Hao et al., 2014) have emerged, which provide many favorable conditions for improving material properties. However, the specific capacitance and energy density of assembled EDLCs cannot compete with pseudocapacitors owing to their inherent electrostatic surface charging mechanism. Therefore, it is an effective way to prepare high-performance composite electrode materials by combining various functional carbon materials and typical metal oxides or conductive polymers.

Among many transition metal oxides, MnO$_2$ with abundant reserves, low toxicity, and simple preparation process, is widely used in oxidation catalyst materials, aqueous batteries, supercapacitors, and other fields (Zhu M. et al., 2018; Li F. et al., 2019; Luo et al., 2019; Wei et al., 2019). Especially in the case of supercapacitors, MnO$_2$ is considered to be one of the most promising electrode materials. Since Lee and Goodenough (1999) reported the pioneering work of amorphous MnO$_2$ electrodes with excellent pseudocapacitive behavior in KCl electrolytes, a large number of efforts have been made to develop high-performance MnO$_2$-based electrode materials. The reasons of the excellent performance of MnO$_2$ can be summed up in two aspects. From the perspective of electrochemical properties, MnO$_2$ displays outstanding characteristics of (a) a high theoretical capacity (1,370 F g^{-1}) referring to the single-electron redox reaction of each manganese atom; (b) a wide potential window (0.9–1.0 V) (Xie Y. et al., 2019); and (c) excellent electrochemical properties in neutral electrolyte, leading to low chemical corrosion of the collector. From the

FIGURE 1 | Ragone plots of various electrochemical energy storage (EES) systems. Reproduced from (Wang J. G. et al., 2015), with permission from Pergamon.

perspective of environmental protection and economy, MnO_2 is abundant in earth, has low price, and is environmentally friendly (Wei et al., 2011). These unique advantages make MnO_2 an ideal choice for pseudocapacitor electrode materials. It is worth noting that MnO_2 contains a variety of crystal structures, including α-, β-, γ-, δ-, and λ-MnO_2; and its energy storage properties are determined by different crystal forms. Research has shown that the chain (Gao et al., 2017) or tunnel (Huang et al., 2019) structure of α-, β-, and γ-MnO_2 with large two-dimensional tunneling structure facilitates electron transfer to provide a relatively high capacitance value. The large surface area of δ-MnO_2 with a layered or sheet-like structure is more favorable for cation intercalation/deintercalation than the amorphous structure. The three-dimensional hinge structure of λ-MnO_2 can provide more active sites for better electrochemical properties (Prélot et al., 2003; Malak-Polaczyk et al., 2010). However, the further development of current MnO_2-based supercapacitors is limited by the drawbacks of MnO_2 electrode materials, such as low conductivity, poor ion diffusion constant, and poor structural stability (Wang J. G. et al., 2015). Therefore, the improvement of active materials mainly involves high reversible capacitance, structural stability, and rapid cation diffusion at high charge/discharge rates. A useful and direct approach is to uniformly modify MnO_2 materials onto layered porous conductive functional carbon materials to construct electrodes (Hu et al., 2018). The carbon materials can be served as a highly conductive and stable current collector, and its interconnection holes are beneficial for ion diffusion, whereas MnO_2 can shorten the transmission distance of ions to prepare a high-performance electrode material.
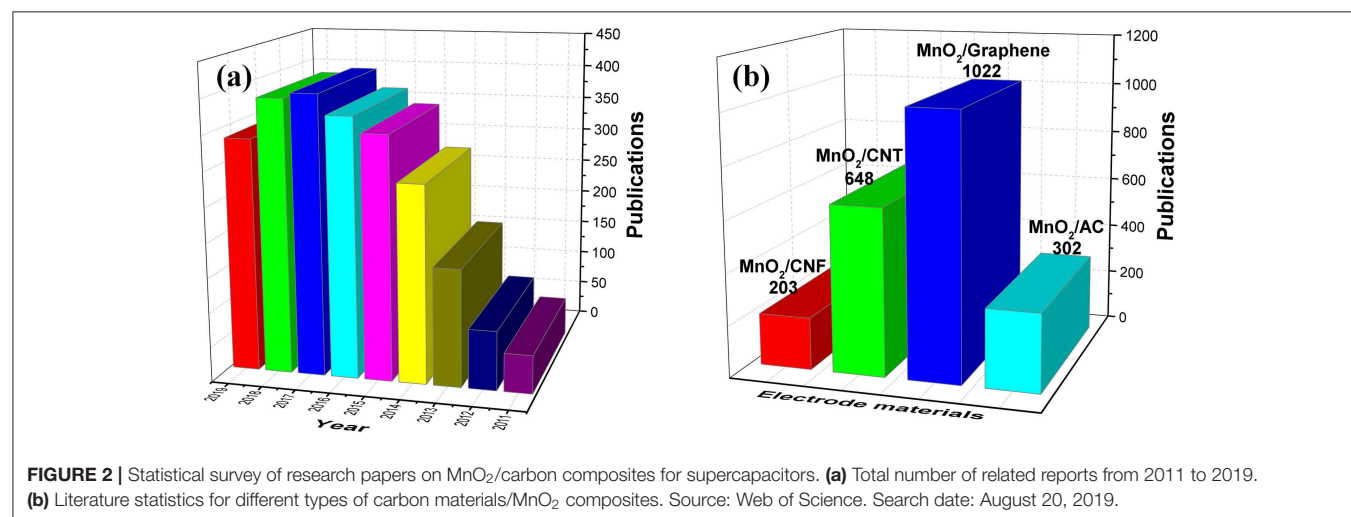
In recent years, a large amount of significant breakthroughs have been made in the design of high-performance MnO_2-based composite materials for application in supercapacitor devices. The number of research papers on MnO_2/carbon composites for supercapacitors recently published is shown in **Figure 2**. In **Figure 2a**, the number of research papers on carbon/MnO_2 composites has remained at a high level, which is still the research focus of electrode materials at present. And as shown in **Figure 2b**, recent work has shown that different types of carbon materials added to MnO_2 material are mainly in forms of graphene and CNTs. This paper summarizes the synthesis strategies of MnO_2/carbon materials with different morphologies and structures. The electrochemical properties and influencing factors of the electrode materials were further discussed. Finally, the remaining challenges of MnO_2/carbon composite supercapacitors are briefly generalized, and an outlook on the possible development directions in the future for designing high-performance MnO_2/carbon materials is also provided.

SYNTHESIS AND PROPERTIES OF MnO_2/CARBON COMPOSITES FOR SUPERCAPACITOR

MnO_2/Carbon Nanotube Composites

CNTs are one-dimensional quantum materials with a hollow tubular structure and excellent electrical conductivity, large specific surface area, and high chemical stability (Lu et al., 2019). From the perspective of the wall structure, it can be divided into single-walled CNTs (SWCNTs) and multi-walled CNTs (MWCNTs), both of which have been widely used in the energy storage. For SWCNTs, the specific surface area can reach 240–1,250 $m^2\ g^{-1}$, and pore size distribution is mostly in the wide range of 3 to 5 nm, with high specific capacitance of 180 $F\ g^{-1}$, power density of 20 $kW\ kg^{-1}$, and energy density of 6.5–7 $Wh\ kg^{-1}$ (Fujiwara et al., 2001). And reduced electrode impedance and increased specific capacitance of SWCNTs can be obtained by the high-temperature heat treatment or addition of surfactants (Byl et al., 2005). For MWCNTs, the specific surface area ($\sim$430 $m^2\ g^{-1}$), specific capacitance ($\sim$180 $F\ g^{-1}$), power density ($\sim$8 $kW\ kg^{-1}$), and energy density ($\sim$0.56 $Wh\ kg^{-1}$) are slightly lower than those for SWCNTs (Fujiwara et al., 2001; Xie et al., 2017). In addition, carbon atoms in the CNTs are sp^2 hybridized, forming a hexagonal network with the surrounding three carbon atoms, and its s orbital composition is relatively large compared with sp^3 hybridization.

FIGURE 2 | Statistical survey of research papers on MnO_2/carbon composites for supercapacitors. **(a)** Total number of related reports from 2011 to 2019. **(b)** Literature statistics for different types of carbon materials/MnO_2 composites. Source: Web of Science. Search date: August 20, 2019.

The carbon atoms in the CNTs adopt sp^2 hybridization, and the surrounding three carbon atoms form a hexagonal network, which is larger than the sp^3 hybrid sulfur orbital composition. This contributed to the high mechanical strength, good flexibility, and excellent corrosion resistance and stability of CNTs that provide advantages for manufacturing flexible electrode. The introduction of carbon–carbon double bond, carboxyl group, hydroxyl group, hydrocarbon bond, and other functional groups on the surface of CNTs can improve their surface activity and help ions in electrolyte to enter into electrode materials. So far, the synthesis of CNTs has entered the commercial stage and production capacity of more than 1,000 tons (Xin and Wei, 2012). As a relatively mature nano-carbon material, the development of CNTs is of great scientific significance in the field of EES.

Considering that the specific capacitance of pure CNTs measuring 20–80 F g^{-1} (Dubey and Guruviah, 2019) is lower than that of other carbon materials (e.g., CNF is 120–370 F g^{-1} and AC is 100–300 F g^{-1}) and acts more like a scaffold (Zhang and Zhao, 2009), scientists wisely combined MnO$_2$ with CNTs to form nanocomposites. This composite material exerts a synergistic effect of electrical/mechanical benefits of CNTs and large pseudocapacitance of MnO$_2$, achieving expected high specific capacity and long cycle durability. The preparation of MnO$_2$/CNT composite electrode materials can be achieved by various synthetic methods such as electrodeposition techniques (Li Q. et al., 2014; Jeong et al., 2019), hydrothermal treatment (Ramesh et al., 2017), microwave-assisted methods (Yan et al., 2009; Li M. et al., 2017), chemical coprecipitation (Subramanian et al., 2006), and thermal decomposition (Liu et al., 2017; Bi et al., 2019). In 2006, amorphous δ-MnO$_2$ and SWCNT composite electrode materials were first studied. As shown in **Figures 3A,B**, Subramanian et al. (2006) successfully prepared a δ-MnO$_2$/SWCNT composite for supercapacitor electrodes using a simple precipitation method. Owing to the synergetic performance of double layer and pseudocapacitance, the δ-MnO$_2$/20 wt% SWCNT composite exhibits an excellent capacitance value of 110 F g^{-1} at 2 A g^{-1} and maintains 75% capacity over 750 cycles. Further studies have found that the CNT content has a significant effect on the cycle life of the material in **Figure 3C**, so the reasonable ratio of CNTs and MnO$_2$ is very critical for the electrochemical performance improvement of the composite. It is proved that the unique structure of CNTs is served as the conductive agent and support material, whereas MnO$_2$ used as a supplier of pseudocapacitors can significantly improve the electrochemical performance of MnO$_2$/CNT composites. This has led to a strong interest in MnO$_2$/CNT composite electrode materials. (Li L. et al., 2019) developed MnO$_2$-MWCNT by hydrothermal treatment directly on Ni foam for adhesive-free electrodes, as shown in **Figure 3D**. It can be seen from **Figure 3E** that ultrathin MnO$_2$ nanosheets were uniformly grown on forest-like MWCNTs, covering the surface of the foamed nickel. The areal density, specific capacitance, and capacitance retention of the binderless electrode material prepared in this manner reached 0.775 mg cm^{-2}, 1,350.42 F g^{-1} at 6.5 A g^{-1}, and 93.9%, respectively (see **Figure 3F**). This derives from the direct and strong contact between the MWCNT and the current collector that achieves

low charge transfer and enhances the electrochemical properties of the composites, indicating that the binderless approach can significantly improve the conductivity of the electrode material. With the great advancement of science and technology and the improvement of people's living needs, flexible and lightweight flexible electronic devices have attracted widespread attention for their soft, deformable, and easy-to-wear properties. To meet these needs, it is necessary to develop an electrode with good flexibility and excellent electrochemical performance. Wang L. et al. (2017) synthesized SWCNTs by low-crystallization hydrothermal treatment, and then mixed they with MnO$_2$ to form an ordered network structure by vacuum filtration (see **Figure 3G**). The results show that the electrochemical properties of the materials can be improved by effectively regulating the regular fiber network structure. As is shown in **Figures 3H,I**, the area specific capacitance is 964 mF cm^{-2}, and the capacity retention rate is 81% of the composite. The assembled hybrid supercapacitors also provide high energy densities of 31.8 μWh cm^{-2} at a power density of 0.815 mW cm^{-2}, implying their great potential applications in flexible device. In addition, this review summarizes the electrochemical performance of some typical MnO$_2$/CNT electrode materials for comparison (see **Table 1**).

MnO$_2$/Graphene Composites

Graphene is a two-dimensional carbon nanomaterial composed of hexagonal carbon atoms in a honeycomb lattice (Huang et al., 2011; Bayle et al., 2015). With its excellent physical and chemical properties, it has shown broad application prospects in the field of energy storage and conversion (Chen P. et al., 2018; Lu et al., 2018). Interest in the study of graphene has not been attenuated after Novoselov and Geim prepared a single layer of graphene by mechanical stripping at room temperature, breaking the prediction that quasi-two-dimensional crystal materials could not exist alone at room temperature (Novoselov et al., 2004). A two-dimensional planar structure of graphene can be regarded as a building unit for constituting other dimensional carbon materials, such as zero-dimensional fullerene, one-dimensional CNTs, and three-dimensional graphite (Geim and Novoselov, 2007). In addition, the three-dimensional graphene structure can also be constructed by its self-assembling or in combination with other materials. Thanks to its two-dimensional sheet structure that can be used to construct three-dimensional electrode materials with controllable structure, it can meet the needs of no conductive agent and binder addition. The excellent electron migration rate can promote electron transport during charging/discharging to improve electrochemical performance of electrode materials. Due to the special structure of graphene, the theoretically excellent characteristics, such as large specific surface area (∼2,630 m^2 g^{-1}), excellent electrical conductivity, and excellent mechanical properties (resistance). Tensile strength of 130 GPa and stiffness of 1.5 × 10^8 psi, and good chemical and thermal stability (Ren et al., 2018) make it a considerable industrial material that most likely to achieves scale application in the short term for EES (Kannappan et al., 2018).

However, the volumetric energy density of most graphene-based electrode materials is very low, resulting in lower energy density of the electrodes. In order to make full use

FIGURE 3 | Transmission electron microscopy (TEM) pictures. **(A)** Pure single-walled carbon nanotube (SWCNT). **(B)** MnO$_2$:20 wt% SWCNT composite. **(C)** Cyclic voltammograms of pure MnO$_2$, pure SWCNT, and MnO$_2$:20 wt% SWCNT composite at a scan rate of 2 mV s^{-1}. Adapted from Subramanian et al. (2006) with permission from Elsevier Inc. **(D)** Production process of MnO$_2$–multi-walled CNT (MWCNT)–Ni foam. **(E)** MnO$_2$ synthesized uniformly on MWCNTs. **(F)** Charge/discharge curves at different current densities of the MnO$_2$–MWCNT–Ni foam composite. Adapted from (Li L. et al., 2019) under the Creative Commons CC license. **(G)** Schematic preparation representation of the flexible all-solid-state δ-MnO$_2$/SWCNT hybrid supercapacitor. **(H)** Cyclic voltammetry curves from 5 to 100 mV s^{-1}. **(I)** Galvanostatic charge/discharge (GCD) curves of MnO$_2$/SWCNT composites at a current density of 0.1 mA cm^{-2} in a 1 M Na$_2$SO$_4$ electrolyte. Reproduced from Wang L. et al. (2017) with permission from the Royal Society of Chemistry.
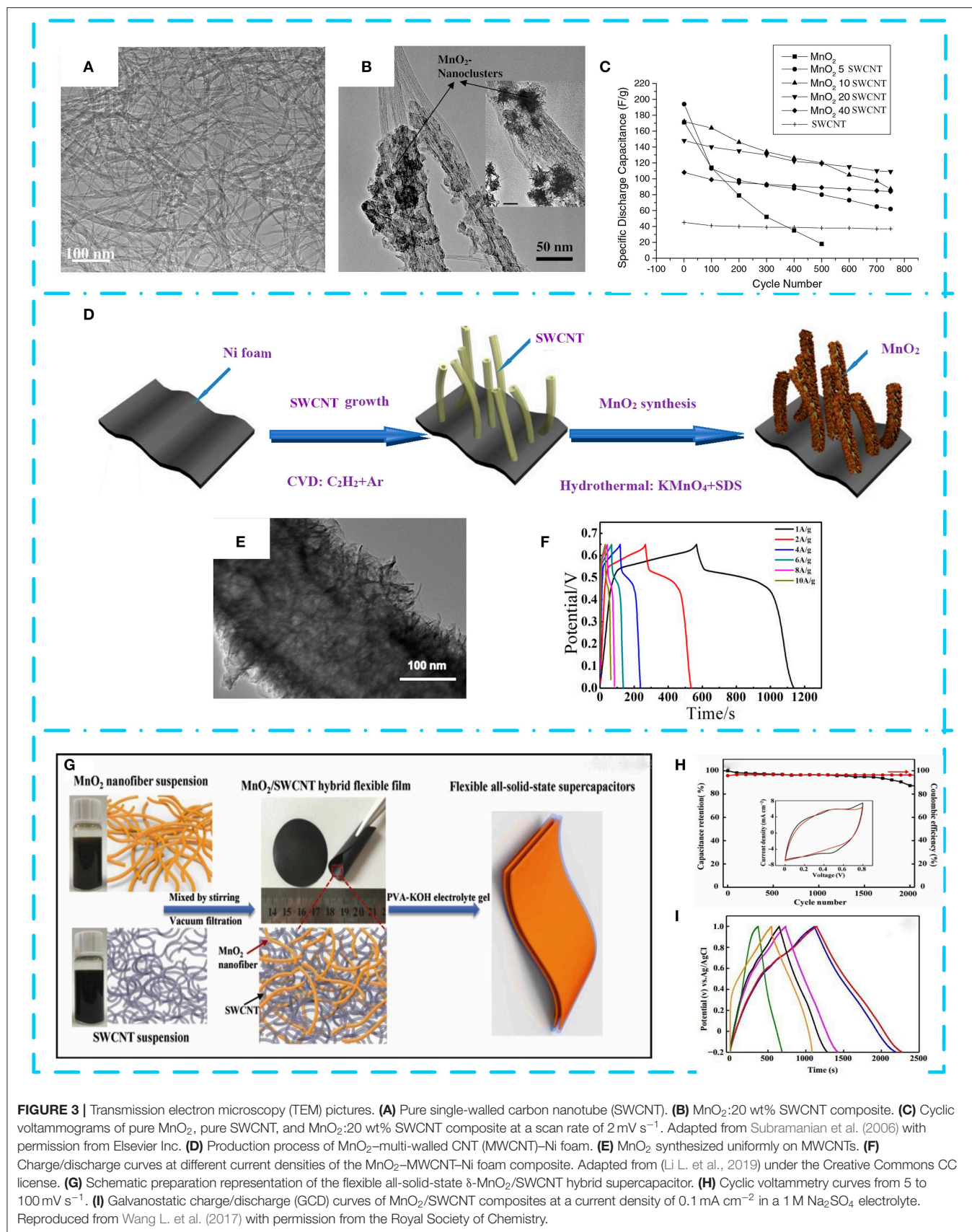
TABLE 1 | Electrochemical performance of various MnO_2/CNT materials.

Material	Electrolyte	Specific capacitance/F g^{-1}	Rate capability/F g^{-1}	Stability (cycles)	References
MnO_2/CNT	0.2 M Na_2SO_4	642 (10 mV s^{-1})	370 (100 mV s^{-1})	~70% (1,000)	Amade et al., 2011
MnO_2/MWCNT	0.5 M Na_2SO_4	276 (3 A g^{-1})	180.5 (9.5 A g^{-1})	91.6% (5,000)	Ramesh et al., 2017
MnO_2/CNT sponge	1 M Na_2SO_4	600 (1 A g^{-1})	430 (10 A g^{-1})	~100% (1,000)	Liu et al., 2017
MnO_2/MWCNT	1 M KCl	251 (0.5 A g^{-1})	–	97% (1,000)	Subagio et al., 2019
MnO_2/CNT	1 M Na_2SO_4	740 (2 mV s^{-1})	503 (100 mV s^{-1})	92% (1,000)	Lv et al., 2012
MnO_2/CNT	0.5 M Na_2SO_4	793 (5 mV s^{-1})	659 (50 mV s^{-1})	97% (5,000)	Li Q. et al., 2014
MnO_2/CNT	1 M Na_2SO_4	740 (10 mV s^{-1})	578 (150 mV s^{-1})	99.5% (800)	Fan et al., 2008a
MWCNT/MnO_2	1 M Na_2SO_4	603.88 (10 mV s^{-1})	405.15 (100 mV s^{-1})	81% (1,000)	Li W. S. et al., 2019
γ-MnO_2/CNT	0.5 M Na_2SO_4	579 (10 mV s^{-1})	422 (150 mV s^{-1})	87.6% (5,000)	Fan et al., 2008b
MnO_2/CNT	0.5 M Na_2SO_4	442.9 (2 mV s^{-1})	180 (100 mV s^{-1})	–	Wang and Igor, 2009
MnO_2/CNT	0.5 M Na_2SO_4	164 (1 A g^{-1})	132 (10 A g^{-1})	–	Xiao et al., 2010
MnO_2/CNT	0.5 M Na_2SO_4	442.9 (2 mV s^{-1})	250 (100 mV s^{-1})	98.9% (1,000)	Zhang et al., 2012
MnO_2/CNT	0.1 M Na_2SO_4	290 (10 mV s^{-1})	145 (200 mV s^{-1})	88.4% (1,000)	Xin and Wei, 2012
MnO_2-doped PANI/CNT	1 M H_2SO_4	1,360 (5 mV s^{-1})	710 (100 mV s^{-1})	>82% (5,000)	Kaushal et al., 2019
MnO_2/SWCNT/SWCNF	0.5 M Na_2SO_4	276 (3 A g^{-1})	180.5 (9.5 A g^{-1})	91.6% (5,000)	Seung Woo et al., 2010
MnO_2/electrospun CNT	6 M KOH	141.7 (5 mV s^{-1})	67 (100 mV s^{-1})	84.9% (1,000)	Wang N. et al., 2011

CNT, carbon nanotube; MWCNT, multi-walled CNT; PANI, polyaniline; SWCNT, single-walled CNT; SWCNF, single-walled carbon nanofiber.

of the excellent properties of graphene, adding MnO_2 to graphene has become a popular choice for most researchers. This can effectively prevent graphene from agglomeration owing to strong van der Waals force by the introduction of MnO_2 between the sheets (Sheng et al., 2016). And the graphene can act as carbon skeleton that exerts an "elastic constraint" to prevent electrochemical dissolution of MnO_2. MnO_2/graphene composites prepared by microwave irradiation, low-temperature hydrothermal treatment, *in situ* reduction method, and electrospinning technology have stimulated their application potential in supercapacitors or other green energy devices. Yan et al. (2010) used a fast and simple microwave radiation method to deposit nanosized MnO_2 on the surface of graphene (see **Figures 4A,B**). The capacitance characteristics of the graphene–MnO_2 composite (78 wt% of MnO_2) show that the measured specific capacitance is 310 F g^{-1} at 2 mV s^{-1} (**Figure 4C**). This is almost three times better than that of pure graphene (104 F g^{-1}) and birnessite MnO_2 (103 F g^{-1}). Interestingly, the weight ratio of MnO_2 in the composite has a great influence on the capacitance performance. As the mass ratio increases from 20 to 78%, the specific capacitance value increases significantly. **Figure 4D** displays schematic preparation process of an ordered MnO_2-GO fiber composite supercapacitor electrode material by electrospinning (Saha et al., 2019). The MnO_2 particles with an average diameter of 260 nm uniformly distributed on the surface of graphene in **Figure 4E**, and the composite exhibited excellent electrochemical performance. The specific capacitance of the sample reached 863.0 F g^{-1} at a current density of 9 A g^{-1}, and the specific capacitance remained 88% of the initial value after 5,000 cycles (**Figure 4F**). By investigating the electrochemical properties, dielectric behavior, and impedance spectra of the samples, it was found that the ordered composites have higher diffusivity and charge mobility than the disordered MnO_2. It is concluded that changing the

crystallinity of MnO_2 with increased electrical conductivity can improve the performance of GO/MnO_2 active materials. As the research progressed, ternary MnO_2 composites have been widely used. For example, Zhu G. et al. (2014) anchored MnO_2 nanoflakes on a graphene–CNT hybrid substrate to form a three-dimensional hybrid material without a binder (**Figures 4G,H**). The hybrid structure completely maintains high conductivity and high surface with increase of volume ratio of CNTs, exhibiting a capacitance value of 251 F g^{-1} at 1 A g^{-1} (see **Figure 4I**). A highly conductive MnO_2–CNT–graphene–Ni-foamed symmetrical supercapacitor delivers an energy density of 1,200 W kg^{-1} at a power density of 29 Wh kg^{-1}. It is worth noting that the crystallinity, micromorphology, and mass ratio of MnO_2 in nanocomposites have a significant effect on the electrochemical performance for supercapacitors. The friendly method under mild conditions is more conducive to the shape control of MnO_2/graphene and the feasibility of expanding production. Furthermore, the control of oxygen-containing functional groups and heteroatom doping of graphene is also a way to manufacture high-performance nanocomposites. The modified nanocomposite can effectively change the electronic properties of graphene and further improve the performance. In addition, this review summarizes the literature on the recently published MnO_2/graphene composites in **Table 2**.

MnO_2/Carbon Nanofiber Composites

CNFs are a type of carbon material that is internally composed of a layer of graphite carbon oriented along the fiber axis. According to different precursors of raw silk, CNFs are mainly divided into three classifications: polyacrylonitrile (PAN)-based carbon fiber, pitch-based carbon fiber, and rayon carbon fiber (Wazir and Kakakhel, 2009). Compared with AC materials, carbon fiber has obvious advantages in performance. The connection of the large, medium, and large number of small holes on the
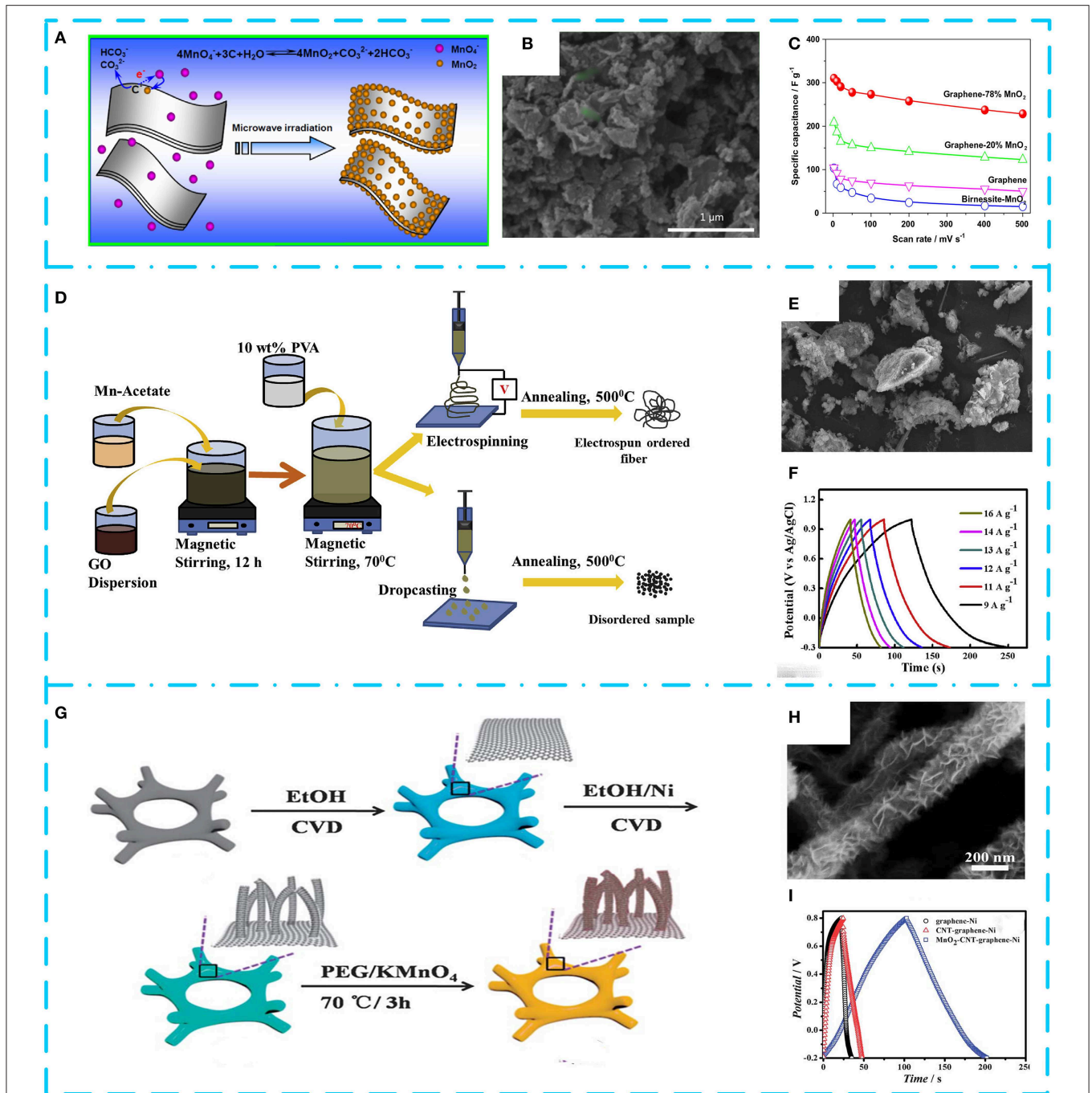
FIGURE 4 | (A) Schematic illustration of the synthesis and electrochemical performance of graphene–MnO₂ composite. **(B)** Low-magnification scanning electron microscopy (SEM) image of graphene−78% MnO₂, showing the preferred growth of MnO₂ near the edges of graphene. **(C)** Specific capacitance of composites at different scan rates of 2, 10, 20, 50, 100, 200, and 500 mV s⁻¹. Reproduced from Yan et al. (2010) with permission from Pergamon. **(D)** Schematic of synthesis procedure. **(E)** SEM image. **(F)** Galvanostatic charge/discharge (GCD) curves at different current densities of MnO₂/graphene−2D composites in 1 M of Na₂SO₄ solution. Adapted from Saha et al. (2019) with permission from Pergamon. **(G)** Schematic illustration. **(H)** SEM images of the fabricated 3D MnO₂-carbon nanotube (CNT)–graphene–Ni hybrids. **(I)** GCD curves of the graphene–Ni, CNT–graphene–Ni, and MnO₂–CNT–graphene–Ni hybrids. Adapted from Zhu G. et al. (2014) with permission from RSC Pub.

surface is very favorable for the transport of the electrolyte and the adsorption of the charges. Moreover, the excellent heat resistance, low thermal expansion, chemical stability, and good

electrical conductivity make them very suitable as electrode materials for supercapacitors (Kim et al., 2019). Generally, CNFs can be prepared by chemical vapor deposition (CVD)

TABLE 2 | Electrochemical performance of various MnO$_2$/graphene materials.

Material	Electrolyte	Specific capacitance/F g^{-1}	Rate capability/F g^{-1}	Stability (cycles)	References
δ-MnO$_2$/graphene	1 M Na$_2$SO$_4$	270 (0.5 A g^{-1})	168 (15 A g^{-1})	90.12% (50,000)	Wang et al., 2019a
MnO$_2$/graphene	1 M KOH	342.8 (0.5 A g^{-1})	111.2 (20 A g^{-1})	90.3% (3,000)	Wang H. et al., 2019
N-doped graphene/MnO$_2$	1 M Na$_2$SO$_4$	411.5 (0.5 A g^{-1})	242 (20 A g^{-1})	88.3% (4,000)	Le et al., 2019
MnO$_2$/GO	1 M Na$_2$SO$_4$	315 (0.5 A g^{-1})	–	∼95% (5,000)	Wu et al., 2010
MnO$_2$/GO	1 M Na$_2$SO$_4$	360.3 (0.5 A g^{-1})	223.6 (5 A g^{-1})	>93% (1,000)	Dai et al., 2014
MnO$_2$/rGO	1 M Na$_2$SO$_4$	759 (2 A g^{-1})	196 (50 A g^{-1})	88% (3,000)	Jadhav et al., 2019
MnO$_2$/rGO	1 M Na$_2$SO$_4$	234.8 (0.1 A g^{-1})	136.9 (5 A g^{-1})	100% (10,000)	Chen Y. et al., 2018
MnO$_2$/graphene	1 M Na$_2$SO$_4$	255 (0.5 A g^{-1})	–	84.5% (10,000)	Zhang Q. et al., 2019
MnO$_2$/graphene	1 M Na$_2$SO$_4$	133 (10 mV s^{-1})	104 (150 mV s^{-1})	75% (10,000)	Amade et al., 2019
Graphene/MnO$_2$/CNTs	1 M Na$_2$SO$_4$	372 (0.5 A g^{-1})	194 (10 A g^{-1})	>90% (3,000)	Cheng et al., 2012
Sponge@rGO@MnO$_2$	1 M Na$_2$SO$_4$	205 (0.1 A g^{-1})	136.9 (5 A g^{-1})	90% (20,000)	Ge et al., 2013

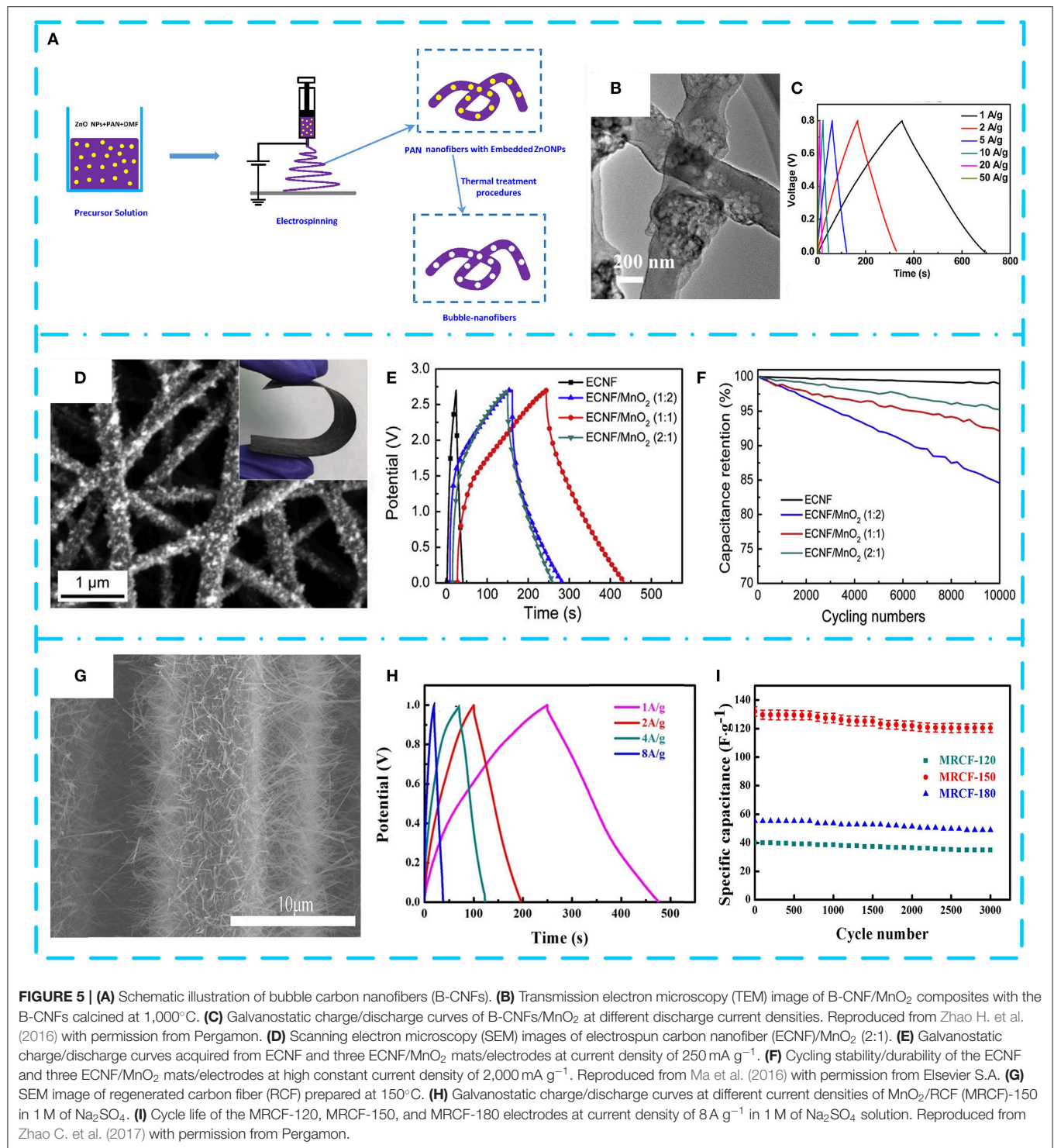*GO, graphene oxide; rGO, reduced GO; CNTs, carbon nanotubes.*

and spinning, using carbon ammonia compounds (including methyl, hexyl, ethyl, and carbon monoxide) as carbon precursors. The ammonium bicarbonate molecules are decomposed at high temperatures under the catalysis of metal catalysts such as iron, diamond, and ruthenium; and carbon atoms diffuse into the graphite layer to form a fibrous structure. The spinning method extrudes the precursor polymer into multiple continuous filaments through wet spinning, gel spinning, baking–melting, dry spinning, and electrostatic spinning, among which electrostatic spinning technology is the most widely applied (Zhang et al., 2015).

Owing to the compact structure, low porosity, and small specific surface area (<10 m^2 g^{-1}) of CNFs in practical applications (Sun et al., 2018), using pure CNFs as electrode materials leads to poor electrochemical performance. Therefore, they can be used as a substrate-carrying MnO$_2$ pseudocapacitor material to improve the electrochemical activity of the electrode, thereby preparing a high-performance composite electrode. Zhao H. et al. (2016) obtained bubble CNFs by exploding PAN at temperatures of 1,000°C in **Figure 5A**. The electrode after decoration with MnO$_2$ nanosheets has a capacitance value of 428 F g^{-1} at 1 A g^{-1} owing to the easy electron transport path of CNFs (**Figures 5B,C**). After 1,500 cycles, the specific capacitance of composites still remained 98.8%. Ma et al. (2016) used electrospun lignin-derived high-graphite electrospun CNF (ECNF; ∼200 nm in diameter and ∼583 m^2 g^{-1} of specific surface area) as the substrate and then decorated with MnO$_2$ nanowhiskers to obtain three kinds of nanocomposites with different weight percentages of MnO$_2$ (**Figure 5D**). The electrochemical performance of the sample with a mass ratio of ECNF and MnO$_2$ of 1:1 is optimal. The supercapacitor device prepared by using the composite as an electrode material has a specific capacitance of 83.3 F g^{-1}, an energy density of 84.3 Wh kg^{-1}, and a power density of 5.72 kW kg^{-1} (**Figures 5E,F**). As shown in **Figure 5G**, an effective solar technology was reported by Zhao C. et al. (2017). They successfully recovered regenerated carbon fiber (RCF) from carbon fiber-reinforced polymer (CFRP), and then the α-MnO$_2$ nanowires were uniformly grown on the surface of

the high temperature-treated RCF. The MnO$_2$/RCF composite (MRCF) prepared by processing CNF at 150°C has an extremely large potential window (1.6 V) and excellent electrochemical performance (specific capacitance is 228.8 F g^{-1} at 1 A g^{-1}, and high cycle stability is ∼91.2% after 3,000 cycles) in **Figures 5H,I**. The asymmetric supercapacitor assembled with the composite as the positive electrode has an operating potential window of 2.0 V and exhibits a high energy density of 22.9 Wh kg^{-1}. There are relatively few studies on MnO$_2$/CNF, and some of the results are shown in **Table 3**. It is found that rationally designing the microstructure of MnO$_2$/CNF composites and enhancing the electrochemical utilization of MnO$_2$ can effectively improve EES.

MnO$_2$/Activated Carbon Composites

AC is a carbon material prepared by pyrolysis and activation of carbon-containing raw materials such as wood, coal, and petroleum coke. It has developed pore structure, large specific surface area, and abundant surface chemical groups (Abioye and Ani, 2015). According to the pore size, it can be classified into three types: macropores (≥50 nm), mesopores (2–50 nm), and micropores (≤2 nm) (Wei et al., 2016). In the energy storage mechanism, large pores are usually used as ion buffers, mesopores (transition pores) are used for efficient ion diffusion, and micropores are used to store charges. Owing to the rich pore structure of AC, its specific surface area can reach up to 3,000 m^2 g^{-1} (Barbieri et al., 2005), which creates favorable conditions for charge storage. AC possesses characteristics of stable chemical properties, abundant sources, wide operating temperature range, simple preparation process, large specific surface area, and environmental protection (Wang Y. et al., 2019). It has been considered to be the most extensive electric double-layer electrode active material in commercial applications. AC for electrodes of electric double-layer capacitors is usually derived from nature, such as charcoal, husks, and biomass, and can also be obtained by carbonized polymers. Generally, the synthesis process of AC is to carbonize a carbonaceous organic precursor in an inert atmosphere at a high temperature and then activate the carbon materials having a high specific surface area by physical or

FIGURE 5 | (A) Schematic illustration of bubble carbon nanofibers (B-CNFs). **(B)** Transmission electron microscopy (TEM) image of B-CNF/MnO_2 composites with the B-CNFs calcined at 1,000°C. **(C)** Galvanostatic charge/discharge curves of B-CNFs/MnO_2 at different discharge current densities. Reproduced from Zhao H. et al. (2016) with permission from Pergamon. **(D)** Scanning electron microscopy (SEM) images of electrospun carbon nanofiber (ECNF)/MnO_2 (2:1). **(E)** Galvanostatic charge/discharge curves acquired from ECNF and three ECNF/MnO_2 mats/electrodes at current density of 250 mA g^{-1}. **(F)** Cycling stability/durability of the ECNF and three ECNF/MnO_2 mats/electrodes at high constant current density of 2,000 mA g^{-1}. Reproduced from Ma et al. (2016) with permission from Elsevier S.A. **(G)** SEM image of regenerated carbon fiber (RCF) prepared at 150°C. **(H)** Galvanostatic charge/discharge curves at different current densities of MnO_2/RCF (MRCF)-150 in 1 M of Na_2SO_4. **(I)** Cycle life of the MRCF-120, MRCF-150, and MRCF-180 electrodes at current density of 8 A g^{-1} in 1 M of Na_2SO_4 solution. Reproduced from Zhao C. et al. (2017) with permission from Pergamon.

chemical activation. Physical activation is usually performed by injecting CO_2 or water vapor at high temperatures to the system, followed by removing precursor uncarbonized substances and selective oxidation of carbides (López Ch et al., 2015). KOH, $ZnCl_2$, and H_3PO_4 are usually used as activators for chemical methods with carbonized substances to selectively react to form

pores and increase specific surface (Abioye and Ani, 2015). According to the double-layer capacitance theory, the specific capacitance of AC is greatly affected by the specific surface area. The initial research hopes to increase specific capacitance by expanding specific surface area and pore volume of carbon materials. However, it is found that the capacitance of electrode

Material	Electrolyte	Specific capacitance/F g^{-1}	Rate capability/F g^{-1}	Stability (cycles)	References
CNF/MnO$_2$	1 M HCl	311 (2 mV s^{-1})	159 (200 mV s^{-1})	97.6% (1,000)	Zhi et al., 2012
CNF/MnO$_2$	6 M KOH	142 (10 mV s^{-1})	–	–	Nataraj et al., 2013
MnO$_2$/catalytically grown CNF	1 M Na$_2$SO$_4$	257 (5 mV s^{-1})	–	105% (1,000)	Zhou et al., 2017
CNFs/MnO$_2$	0.1 M Na$_2$SO$_4$	557 (1 A g^{-1})	186 (30 A g^{-1})	94% (1,500)	Wang J. G et al., 2011
CNFs/MnO$_2$	0.5 M Na$_2$SO$_4$	365 (1 A g^{-1})	–	95.3% (1,000)	Wang et al., 2013
MnO$_2$/CNF	0.1 M Na$_2$SO$_4$	374 (2 mV s^{-1})	198 (100 mV s^{-1})	94% (1,000)	Wang J. G. et al., 2012
CNT/CNF/MnO$_2$	1 M Na$_2$SO$_4$	517 (5 mV s^{-1})	–	75% (1,000)	Wang T. et al., 2015

CNF, carbon nanofiber.

materials is not linearly related to the specific surface area. Even if the specific surface area increases a lot, the increase of specific capacitance is still limited. Moreover, these shortcomings will in turn reduce the energy density and power density of AC electrode.

In order to further obtain high energy density and volume density, typical pseudocapacitive materials such as MnO$_2$ are increasingly anchored on AC to obtain ideal electrode materials. Chen M. D. et al. (2014) selected cotton stalk as carbon precursor and synthesized an amorphous AC material with 1,481 m^2 g^{-1} of specific surface area using H$_3$PO$_4$ as activator by one-step chemical activation. After that, electrolytic MnO$_2$/AC composites with different contents of MnO$_2$ were prepared, as shown in **Figure 6A**. The galvanostatic charge test confirmed that the composite with 5% MnO$_2$ (labeled as AC4) has optimum specific capacitance (169 F g^{-1}) and excellent cycle life (99.2% after 500 cycles), as shown in **Figures 6B,C**. With the deepening research, Zhang J. et al. (2019) proposed a novel high-voltage anode electrodeposition technique to deposit graded MnO$_2$ on AC cloth (**Figure 6D**). Interestingly, it was found that the AC cloth was activated to have a significant improvement in the conductivity and hydrophilicity of the composite electrode. It can be seen from **Figure 6E** that benefiting from the high conductivity of the closely contacted AC cloth/MnO$_2$ interface, the electrode exhibits a specific capacitance of 400 F g^{-1} in 1 M of Na$_2$SO$_4$ at 0.5 A g^{-1} in an asymmetric supercapacitor, and the impressive volumetric energy density reaches 3.82 mWh cm^{-3}. **Figure 6F** shows the good flexibility and mechanical properties of the composite. In **Figures 6G,H**, Li H. et al. (2019) combine AC fibers with MnO$_2$ to form electrodes with excellent flexibility and excellent capacitance properties. The area ratio of the composite material is as high as 410 mF cm^{-2}, delivering a high energy density of 36 μWh cm^{-2} and a high power density of 726 μW cm^{-2} (**Figure 6I**). Integrated devices with multiple electrodes can successfully illuminate light-emitting diodes, showing great potential applications. Finally, it is found that the perfect pore structure and proper surface modification that can function as a fast transfer ion and increase the wettability of the electrode surface are beneficial for suitable pore size distribution. Moreover, the presence of the AC can prevent agglomeration of MnO$_2$ and maximize the MnO$_2$ pseudocapacitance. **Table 4** summarizes the electrochemical performance of some representative MnO$_2$/AC composites. It shows that MnO$_2$/AC composites, as an environmentally friendly supercapacitor electrode material, have become a preferred choice for researchers.

SUMMARY AND OUTLOOK

This review summarizes the research achievements in synthesis methods and electrochemical performance of MnO$_2$/carbon composites for supercapacitors in recent years. In this system, MnO$_2$ provides a source of high specific capacitance and high energy density, while carbon materials ensure excellent cycle performance and high power density. Impressively, various functional carbon materials exhibit their own excellent physical and chemical properties in different dimensions, which provides feasibility to rationally optimize the microstructure and maximization of electrochemical properties of MnO$_2$/carbon electrode materials. Among these carbon substrates, one-dimensional carbon materials of CNTs and CNFs can provide high-speed diffusion and shorten ion diffusion paths owing to their high conductivity and good mechanical properties, becoming the preferred choice for flexible supercapacitors. Two-dimensional carbon materials represented by graphene are regarded as ideal conductive substrates for their high specific surface area, ultra-low density, and good electrical conductivity. Other AC materials with typical three-dimensional structure are widely used in preparing energy storage devices with high energy density due to their large number of microporous structures and rich functional groups. In general, carbon nanomaterial with excellent porous structure and high conductivity can maximize the electrochemical performance of MnO$_2$. Orderly and tidy channels (such as mesoporous carbon) can accelerate the transport of electrolyte ions and make it easier to enter MnO$_2$. Meanwhile, enhancing the degree of graphitization of carbon materials (such as CNTs and graphene) is conducive to the improvement of conductivity to ensure rapid transfer of charge. In recent years, numerous efforts have been made to explore high-performance MnO$_2$/carbon composites for supercapacitors, and exciting improvements have been achieved. However, there are still remaining several key drawbacks in those composites, such as the lack of ordered pore

FIGURE 6 | (A) Scanning electron microscopy (SEM) images of AC4. **(B)** Galvanostatic charge/discharge curves of AC4 at 1.0 A g^{-1}. **(C)** Charge–discharge cycling stability of AC4 at current density of 2 A g^{-1}. Reproduced from Chen M. D. et al. (2014) with permission from Maney Publishing. **(D)** Cross-sectional SEM image of MnO$_2$/AC cloth-300. **(E)** Variations of the capacitance with current densities. **(F)** Schematic representation of the as-prepared electrode. Reproduced from (Zhang J. et al., 2019) with permission from Elsevier BV. **(G)** The corresponding energy-dispersive X-ray spectroscopy (EDS) elemental maps of Mn, O, and C. **(H)** Structure and electrochemical performance. **(I)** Charge–discharge curves at 0.1 mA cm^{-2} under different bending states of the MnO$_2$@ACF-6. Reproduced from (Li H. et al., 2019) with permission from Elsevier.

channels in the carbon substrate (Wang T. et al., 2015), the violent volume expansion and low electrochemical utilization rate of MnO$_2$ (Lei et al., 2012; Sun et al., 2017), and optimization of the composite structure (Zhang Q. Z. et al., 2018).

Faced with these practical challenges and obstacles, we believe that much more efforts should be focused on developing new-generation MnO$_2$/carbon composites that can better meet the energy storage requirements and standards of advanced supercapacitors in the future. Therefore, we suggest that future research trends may focus on the following aspects:

(1) For MnO$_2$/CNTs or CNFs, a carbon substrate with the optimal pore size distribution and specific surface area should be constructed to increase the specific capacity and power density of the supercapacitor; improve the poor surface wettability of CNTs by surface modification, ultrasound, and other treatments to ensure uniformity of MnO$_2$ deposition; and optimize the design of flexible and foldable CNF substrates that meet different requirements without sacrificing stable power output and long cycle stability.

(2) For MnO$_2$/AC, the low-mass load problem of MnO$_2$ should be improved without sacrificing the power of the

TABLE 4 | Electrochemical performance of various MnO$_2$/CNT material.

Material	Electrolyte	Specific capacitance/F g^{-1}	Rate capability/F g^{-1}	Stability (cycles)	References
AC/MnO$_2$	6 M KOH	193 (0.2 A g^{-1})	154 (2 A g^{-1})	77.8% (1,500)	Liu et al., 2015
Porous AC/MnO$_2$	6 M KOH	258 (1 A g^{-1})	235 (20 A g^{-1})	93.6% (10,000)	Kong et al., 2019
MnO$_2$/AC cloth	1 M Na$_2$SO$_4$	257 (5 mV s^{-1})	–	94.2% (5,000)	Shen et al., 2019
AC/MnO$_2$	1 M Na$_2$SO$_4$	297.8 (0.2 A g^{-1})	155 (20 A g^{-1})	94.8% (1,000)	Kim et al., 2015
AC/MnO$_2$	1 M Na$_2$SO$_4$	90.5 (5 mV s^{-1})	–	91.3% (1,000)	Kim et al., 2013
MnO$_2$/spherical AC	0.1 M Na$_2$SO$_4$	357 (1 A g^{-1})	–	93% (3,000)	Li Z. et al., 2014

CNF, carbon nanofiber; AC, activated carbon.

composite material to balance the overall performance, effectively exerting the coordination performance of MnO$_2$ and carbon materials.

(3) For MnO$_2$/graphene, MnO$_2$ should be deposited more uniformly on the surface of graphene and should establish an intimate connection by the new composite technology to prevent the damage of composite structure and improve the rate capability and cycle stability.

(4) MnO$_2$ should be combined with economical and green carbon materials to develop light, low-price, and environmentally friendly composite electrode materials.

AUTHOR CONTRIBUTIONS

All authors listed have made a substantial, direct and intellectual contribution to the work, and approved it for publication.

FUNDING

REFERENCES

Abioye, A. M., and Ani, F. N. (2015). Recent development in the production of activated carbon electrodes from agricultural waste biomass for supercapacitors: a review. *Renew. Sust. Energ. Rev.* 52, 1282–1293. doi: 10.1016/j.rser.2015.07.129

Amade, R., Jover, E., Caglar, B., Mutlu, T., and Bertran, E. (2011). Optimization of MnO$_2$/vertically aligned carbon nanotube composite for supercapacitor application. *J. Power Sources* 196, 5779–5783. doi: 10.1016/j.jpowsour.2011.02.029

Amade, R., Muyshegyan-Avetisyan, A., González, J. M., Pino, A. P., György, E., Pascual, E., et al. (2019). Super-capacitive performance of manganese dioxide/graphene nano-walls electrodes deposited on stainless steel current collectors. *Materials* 12:483. doi: 10.3390/ma12030483

Barbieri, O., Hahn, M., Herzog, A., and Kötz, R. (2005). Capacitance limits of high surface area activated carbons for double layer capacitors. *Carbon* 43, 1303–1310. doi: 10.1016/j.carbon.2005.01.001

Bayle, M., Reckinger, N., Huntzinger, J. R., Felten, A., Bakaraki, A., Lan Landois, P., et al. (2015). Dependence of the Raman spectrum characteristics on the number of layers and stacking orientation in few-layer graphene. *Phys. Status Solidi* 252, 2375–2379. doi: 10.1002/pssb.201552204

Bi, T., Fang, H., Jiang, J., He, X., Zhen, X., Yang, H., et al. (2019). Enhance supercapacitive performance of MnO$_2$/3D carbon nanotubes-graphene as a binder-free electrode. *J. Alloys Compd.* 30, 759–766. doi: 10.1016/j.jallcom.2019.02.117

Borenstein, A., Hanna, O., Attias, R., Luski, S., Brousse, T., and Aurbach, D. (2017). Carbon-based composite materials for supercapacitor electrodes: a review. *J. Mater. Chem.* 5, 12653–12672. doi: 10.1039/C7TA00863E

Byl, O., Liu, J., and Yates, J. T. (2005). Etching of carbon nanotubes by ozone-a surface area study. *Langmuir* 21, 4200–4204. doi: 10.1021/la040132w

Candelaria, S. L., Shao, Y., Zhou, W., Li, X., Xiao, J., Zhang, J. G., et al. (2012). Nanostructured carbon for energy storage and conversion. *Nano Energy* 1, 195–220. doi: 10.1016/j.nanoen.2011.11.006

Chen, M. D., Wumaie, T., Li, W. L., Song, H. H., and Song, R. R. (2014). Electrochemical performance of cotton stalk based activated carbon electrodes modified by MnO$_2$ for supercapacitor. *Mater. Technol.* 30, A2–A7. doi: 10.1179/1753555714Y.0000000241

Chen, P., Yang, C., He, Z., and Guo, K. (2018). One-pot facile route to fabricate the precursor of sulfonated graphene/N-doped mesoporous carbons composites for supercapacitors. *J. Mater. Sci.* 54, 4180–4191. doi: 10.1007/s10853-018-3122-6

Chen, Y., Zhang, J., Li, M., Yang, C., Zhang, L., Wang, C., et al. (2018). Strong interface coupling and few-crystalline MnO$_2$/Reduced graphene oxide composites for supercapacitors with high cycle stability. *Electrochim. Acta* 292, 115–124. doi: 10.1016/j.electacta.2018.09.131

Cheng, Y., Lu, S., Zhang, H., Varanasi, C. V., and Liu, J. (2012). Synergistic effects from graphene and carbon nanotubes enable flexible and robust electrodes for high-performance supercapacitors. *Nano Lett.* 12, 4206–4211. doi: 10.1021/nl301804c

Conway, B. E. (1999). *Electrochemical Supercapacitors: Scientific Fundamentals and Technological Applications.* NewYork, NY: Springer. doi: 10.1007/978-1-4757-3058-6

Dai, K., Lu, L., Liang, C., Dai, J., Liu, Q., Zhang, Y., et al. (2014). *In situ* assembly of MnO$_2$ nanowires/graphene oxide nanosheets composite with high specific capacitance. *Electrochim. Acta* 116, 111–117. doi: 10.1016/j.electacta.2013.11.036

Díaz-Delgado, R., and Doherty, A. P. (2016). Carbons, ionic liquids, and quinones for electrochemical capacitors. *Front. Mater.* 3:18. doi: 10.3389/fmats.2016.00018

Dubey, R., and Guruviah, V. (2019). Review of carbon-based electrode materials for supercapacitor energy storage. *Ionics* 25, 1419–1445. doi: 10.1007/s11581-019-02874-0

Fan, Z., Chen, J., Zhang, B., Liu, B., Zhong, X., and Kuang, Y. (2008a). High dispersion of γ-MnO$_2$ on well-aligned carbon nanotube arrays and its application in supercapacitors. *Diamond Relat. Mater.* 17, 1943–1948. doi: 10.1016/j.diamond.2008.04.015

Fan, Z., Chen, J., Zhang, B., Sun, F., Liu, B., and Kuang, Y. (2008b). Electrochemically induced deposition method to prepare γ-MnO$_2$/multi-walled carbon nanotube composites as electrode material in supercapacitors. *Mater. Res. Bull.* 43, 2085–2091. doi: 10.1016/j.materresbull.2007.09.015

Faraji, S., and Ani, F. N. (2015). The development supercapacitor from activated carbon by electroless plating-A review. *Renew. Sust. Energ. Rev.* 42, 823–834. doi: 10.1016/j.rser.2014.10.068

Fujiwara, A., Ishii, K., Suematsu, H., Kataura, H., Maniwa, Y., Suzuki, S., et al. (2001). Gas adsorption in the inside and outside of single-walled carbon nanotubes. *Chem. Phys. Lett.* 336, 205–211. doi: 10.1016/S0009-2614(01)00111-7

Gao, F., Tang, X., Yi, H., Chao, C., Na, L., Li, J., et al. (2017). *In-situ* DRIFTS for the mechanistic studies of NO oxidation over α-MnO$_2$, β-MnO$_2$ and γ-MnO$_2$ catalysts. *Chem. Eng. J.* 322, 525–537. doi: 10.1016/j.cej.2017.04.006

Ge, J., Yao, H. B., Hu, W., Yu, X. F., Yan, Y. X., Mao, L. B., et al. (2013). Facile dip coating processed graphene/MnO$_2$ nanostructured sponges as high performance supercapacitor electrodes. *Nano Energy* 2, 505–513. doi: 10.1016/j.nanoen.2012.12.002

Geim, A. K., and Novoselov, K. S. (2007). The rise of graphene. *Nat. Mater.* 6, 183–191. doi: 10.1038/nmat1849

Hao, P., Zhao, Z., Tian, J., Li, H., Sang, Y., Yu, G., et al. (2014). Hierarchical porous carbon aerogel derived from bagasse for high performance supercapacitor electrode. *Nanoscale* 6, 12120–12129. doi: 10.1039/C4NR03574G

He, Y., Chen, W., Gao, C., Zhou, J., Li, X., and Xie, E. (2013). An overview of carbon materials for flexible electrochemical capacitors. *Nanoscale* 5, 8799–8820. doi: 10.1039/c3nr02157b

Hu, Y., Wu, Y., and Wang, J. (2018). Manganese-oxide-based electrode materials for energy storage applications: how close are we to the theoretical capacitance? *Adv. Mater.* 30:e1802569. doi: 10.1002/adma.201802569

Huang, J., Dai, Y., Singewald, K., Liu, C. C., Saxena, S., and Zhang, H. (2019). Effects of MnO$_2$ of different structures on activation of peroxymonosulfate for bisphenol A degradation under acidic conditions. *Chem. Eng. J.* 370, 906–915. doi: 10.1016/j.cej.2019.03.238

Huang, X., Yin, Z., Wu, S., Qi, X., He, Q., Zhang, Q., et al. (2011). Graphene-based materials: synthesis, characterization, properties, and applications. *Small* 7, 1876–1902. doi: 10.1002/smll.201002009

Jadhav, S., Kalubarme, R. S., Terashima, C., Kale, B. B., Godbole, V., Fujishima, A., et al. (2019). Manganese dioxide/reduced graphene oxide composite an electrode material for high-performance solid state supercapacitor. *Electrochim. Acta* 299, 34–44. doi: 10.1016/j.electacta.2018.12.182

Jeong, J. H., Park, J. W., Lee, D. W., Baughman, R. H., and Kim, S. J. (2019). Electrodeposition of α-MnO$_2$/γ-MnO$_2$ on carbon nanotube for yarn supercapacitor. *Sci. Rep.* 9:11271. doi: 10.1038/s41598-019-47744-x

Kannappan, S., Hao, Y., Kaliyappan, K., Manian, R. K., Pandian, A. S., Lee, Y. S., et al. (2018). Thiolated-graphene-based supercapacitors with high energy density and stable cycling performance. *Carbon* 134, 326–333. doi: 10.1016/j.carbon.2018.02.036

Kaushal, I., Sharma, A. K., Saharan, P., Sadasivuni, K. K., and Duhan, S. (2019). Superior architecture and electrochemical performance of MnO$_2$ doped PANI/CNT graphene fastened composite. *J. Porous Mat.* 26, 1287–1296. doi: 10.1007/s10934-019-00728-8

Kim, C. H., Yang, C. M., Kim, Y. A., and Yang, K. S. (2019). Pore engineering of nanoporous carbon nanofibers toward enhanced supercapacitor performance. *Appl. Surf. Sci.* 497:143693. doi: 10.1016/j.apsusc.2019.143693

Kim, M., Hwang, Y., Min, K., and Kim, J. (2013). Introduction of MnO$_2$ nanoneedles to activated carbon to fabricate high-performance electrodes as electrochemical supercapacitors. *Electrochim. Acta* 113, 322–331. doi: 10.1016/j.electacta.2013.09.058

Kim, S., Lee, J., Kang, J. S., Jo, K., Kim, S., Sung, Y. E., et al. (2015). Lithium recovery from brine using a k-MnO$_2$/activated carbon hybrid supercapacitor system. *Chemosphere* 125, 50–56. doi: 10.1016/j.chemosphere.2015.01.024

Kong, S., Jin, B., Quan, X., Zhang, G., Guo, X., Zhu, Q., et al. (2019). MnO$_2$ nanosheets decorated porous active carbon derived from wheat bran for high-performance asymmetric supercapacitor. *J. Electroanal. Chem.* 850:113412. doi: 10.1016/j.jelechem.2019.113412

Le, Q., Huang, M., Wang, T., Liu, X., Sun, L., Guo, X., et al. (2019). Biotemplate derived three dimensional nitrogen doped graphene@MnO$_2$ as bifunctional material for supercapacitor and oxygen reduction reaction catalyst. *J. Colloid Interface Sci.* 544, 155–163. doi: 10.1016/j.jcis.2019.02.089

Lee, H., and Goodenough, J. B. (1999). Supercapacitor behavior with KCl electrolyte. *J. Solid State Chem.* 144, 220–223. doi: 10.1006/jssc.1998.8128

Lei, Z., Shi, F., and Lu, L. (2012). Incorporation of MnO$_2$-coated carbon nanotubes between graphene sheets as supercapacitor electrode. *ACS Appl. Mater. Interfaces* 4, 1058–1064. doi: 10.1021/am2016848

Li, F., Wang, J., Liu, L., Qu, J., Li, Y., Bandari, V. K., et al. (2019). Self-assembled flexible and integratable 3D microtubular asymmetric supercapacitors. *Adv. Sci.* 6:1901051. doi: 10.1002/advs.201901051

Li, H., Liang, J., Li, H., Zheng, X., Tao, Y., Huang, Z. H., et al. (2019). Activated carbon fibers with manganese dioxide coating for flexible fiber supercapacitors with high capacitive performance. *J. Energy Chem.* 31, 95–100. doi: 10.1016/j.jechem.2018.05.008

Li, L., Chen, L., Qian, W., Xie, F., and Dong, C. (2019). Directly grown multiwall carbon nanotube and hydrothermal MnO$_2$ composite for high-performance supercapacitor electrodes. *Nanomaterials* 9:703. doi: 10.3390/nano9050703

Li, M., Chen, Q., and Zhan, H. (2017). Ultrathin manganese dioxide nanosheets grown on partially unzipped nitrogen-doped carbon nanotubes for high-performance asymmetric supercapacitors. *J. Alloys Compd.* 702, 236–243. doi: 10.1016/j.jallcom.2017.01.244

Li, Q., Lu, X. F., Xu, H., Tong, Y. X., and Li, G. R. (2014). Carbon/MnO$_2$ double-walled nanotube arrays with fast ion and electron transmission for high-performance supercapacitors. *ACS Appl. Mater. Interfaces* 6, 2726–2733. doi: 10.1021/am405271q

Li, W. S., Chang, M. L., Chuang, K. C., Li, Y. S., Luo, J. D., and Cheng, H. C. (2019). Electrochemical properties of CNT/MnO$_2$ hybrid nanostructure with low-temperature hydrothermal synthesis as high-performance supercapacitor. *J. Electrochem. Soc.* 166, A2194–A2198. doi: 10.1149/2.1551910jes

Li, Z., Liu, Z., Li, D., Li, B., Li, Q., Huang, Y., et al. (2014). Facile synthesis of α-MnO$_2$ nanowires/spherical activated carbon composite for supercapacitor application in aqueous neutral electrolyte. *J. Mater. Sci.-Mater. Electron.* 26, 353–359. doi: 10.1007/s10854-014-2407-z

Liang, M., and Xin, H. (2015). Microwave to terahertz: characterization of carbon-based nanomaterials. *IEEE Microw. Mag.* 15, 40–51. doi: 10.1109/MMM.2013.2288708

Liu, R., Liu, E., Ding, R., Liu, K., Teng, Y., Luo, Z., et al. (2015). Facile *in-situ* redox synthesis of hierarchical porous activated carbon@MnO$_2$ core/shell nanocomposite for supercapacitors. *Ceram. Int.* 41, 12734–12741. doi: 10.1016/j.ceramint.2015.06.106

Liu, Y., Zhou, X., Liu, R., Li, X., Bai, Y., and Yuan, G. (2017). Preparation of three-dimensional compressible MnO$_2$@carbon nanotube sponges with enhanced supercapacitor performance. *N. J. Chem.* 41, 14906–14913. doi: 10.1039/C7NJ03323K

López Ch, L. T., Chejne, F., and Bhatia, S. K. (2015). Effect of activating agents: flue gas and CO$_2$ on the preparation of activated carbon for methane storage. *Energy Fuels* 29, 6296–6305. doi: 10.1021/acs.energyfuels.5b01438

Lu, S., Guo, K. K., Xie, Y., and Ning, J. (2018). Ordered mesoporous carbons loading on sulfonated graphene by multi-components Co-assembly for supercapacitor applications. *Energy Technol.* 6, 1975–1985. doi: 10.1002/ente.201800116

Lu, Z., Raad, R., Safaei, F., Xi, J., Liu, Z., and Foroughi, J. (2019). Carbon nanotube based fiber supercapacitor as wearable energy storage. *Front. Mater.* 6:138. doi: 10.3389/fmats.2019.00138

Luo, S., Xie, L., Han, F., Wei, W., Huang, Y., Zhang, H., et al. (2019). Nanoscale parallel circuitry based on interpenetrating conductive sssembly for flexible and high-power zinc ion battery. *Adv. Funct. Mater.* 29:1901336. doi: 10.1002/adfm.201901336

Lv, P., Zhang, P., Feng, Y., Li, Y., and Feng, W. (2012). High-performance electrochemical capacitors using electrodeposited MnO$_2$ on carbon nanotube array grown on carbon fabric. *Electrochim. Acta* 78, 515–523. doi: 10.1016/j.electacta.2012.06.085

Ma, X., Kolla, P., Zhao, Y., Smirnova, A. L., and Fong, H. (2016). Electrospun lignin-derived carbon nanofiber mats surface-decorated with MnO$_2$ nanowhiskers as binder-free supercapacitor electrodes with high performance. *J. Power Sources* 325, 541–548. doi: 10.1016/j.jpowsour.2016.06.073

Malak-Polaczyk, A., Matei-Ghimbeu, C., Vix-Guterl, C., and Frackowiak, E. (2010). Carbon/λ-MnO$_2$ composites for supercapacitor electrodes. *J. Solid State Chem.* 183, 969–974. doi: 10.1016/j.jssc.2010.02.015

Nataraj, S. K., Song, Q., Al-Muhtaseb, S. A., Dutton, S. E., Zhang, Q., and Sivaniah, E. (2013). Thin, flexible supercapacitors made from carbon nanofiber

electrodes decorated at room temperature with manganese oxide nanosheets. *J. Nanomater.* 2013, 1–6. doi: 10.1155/2013/272093

Novoselov, K. S., Geim, A. K., Morozov, S. V., Jiang, D., Zhang, Y., Dubonos, S. V., et al. (2004). Electric field effect in atomically thin carbon films. *Science* 306, 666–669. doi: 10.1126/science.1102896

Palchoudhury, S., Ramasamy, K., Gupta, R. K., and Gupta, A. (2019). Flexible supercapacitors: a materials perspective. *Front. Mater.* 5:83. doi: 10.3389/fmats.2018.00083

Peng, S., Li, L., Yoong, J. L. K., Tian, L., Srinivasan, M., Adams, S., et al. (2016). Electrospun carbon nanofibers and their hybrid composites as advanced materials for energy conversion and storage. *Nano Energy* 22, 361–395. doi: 10.1016/j.nanoen.2016.02.001

Prélot, B., Poinsignon, C., Thomas, F., Schouller, E., and Villiéras, F. (2003). Structural-chemical disorder of manganese dioxides: 1. Influence on surface properties at the solid-electrolyte interface. *J. Colloid Interface Sci.* 257, 77–84. doi: 10.1016/S0021-9797(02)00013-9

Qian, W., Xu, G., Fei, W., Chao, Z., Cui, C., Zhao, M., et al. (2012). Carbon nanotubes for supercapacitors:consideration of cost and chemical vapor deposition techniques. *J. Energy Chem.* 21, 233–240. doi: 10.1016/S1003-9953(11)60358-7

Ramesh, S., Kim, H. S., Haldorai, Y., Han, Y. K., and Kim, J. H. (2017). Fabrication of nanostructured MnO$_2$/carbon nanotube composite from 3D precursor complex for high-performance supercapacitor. *Mater. Lett.* 196, 132–136. doi: 10.1016/j.matlet.2017.03.044

Ren, S., Rong, P., and Yu, Q. (2018). Preparations, properties and applications of graphene in functional devices: a concise review. *Ceram. Int.* 44, 11940–11955. doi: 10.1016/j.ceramint.2018.04.089

Saha, S., Maji, P., Pethsangave, D. A., Roy, A., Ray, A., Some, S., et al. (2019). Effect of morphological ordering on the electrochemical performance of MnO$_2$-graphene oxide composite. *Electrochim. Acta* 317, 199–210. doi: 10.1016/j.electacta.2019.05.148

Salinas-Torres, D., Ruiz-Rosas, R., Morallón, E., and Cazorla-Amorós, D. (2019). Strategies to enhance the performance of electrochemical capacitors based on carbon materials. *Front. Mater.* 6:115. doi: 10.3389/fmats.2019.00115

Seung Woo, L., Junhyung, K., Shuo, C., Hammond, P. T., and Yang, S. H. (2010). Carbon nanotube/manganese oxide ultrathin film electrodes for electrochemical capacitors. *ACS Nano* 4, 3889–3896. doi: 10.1021/nn100681d

Shen, H., Zhang, Y., Song, X., Liu, Y., Wang, H., Duan, H., et al. (2019). Facile hydrothermal synthesis of actiniaria-shaped α-MnO$_2$/activated carbon and its electrochemical performances of supercapacitor. *J. Alloys Compd.* 770, 926–933. doi: 10.1016/j.jallcom.2018.08.228

Sheng, L., Jiang, L., Wei, T., and Fan, Z. (2016). High volumetric energy density asymmetric supercapacitors based on well-balanced graphene and graphene-MnO$_2$ electrodes with densely stacked architectures. *Small* 12, 5217–5227. doi: 10.1002/smll.201601722

Shi, X., Zheng, S., Wu, Z. S., and Bao, X. (2018). Recent advances of graphene-based materials for high-performance and new-concept supercapacitors. *J. Energy Chem.* 27, 25–42. doi: 10.1016/j.jechem.2017.09.034

Snook, G. A., Kao, P., and Best, A. S. (2011). Conducting-polymer-based supercapacitor devices and electrodes. *J. Power Sources* 196, 1–12. doi: 10.1016/j.jpowsour.2010.06.084

Subagio, A., Hakim, Y. A., Ristiawan1, M. W., Kholil1, M. A., and Priyono (2019). Structural and morphological properties of MnO$_2$/MWCNT composite grown using the hydrothermal method for supercapacitor application. *J. Inorg. Organomet. Polym. Mater.* 14, 9936–9947. doi: 10.20964/2019.10.52

Subramanian, V., Zhu, H., and Wei, B. (2006). Synthesis and electrochemical characterizations of amorphous manganese oxide and single walled carbon nanotube composites as supercapacitor electrode materials. *Electrochem. Commun.* 8, 827–832. doi: 10.1016/j.elecom.2006.02.027

Sun, J., Cui, B., Chu, F., Yun, C., He, M., Li, L., et al. (2018). Printable Nanomaterials for the fabrication of high-performance supercapacitors. *Nanomaterials* 8:528. doi: 10.3390/nano8070528

Sun, P., Yi, H., Peng, T., Jing, Y., Wang, R., Wang, H., et al. (2017). Ultrathin MnO$_2$ nanoflakes deposited on carbon nanotube networks for symmetrical supercapacitors with enhanced performance. *J. Power Sources* 341, 27–35. doi: 10.1016/j.jpowsour.2016.11.112

Tajik, S., Dubal, D. P., Gomez-Romero, P., Yadegari, A., Rashidi, A., Nasernejad, B., et al. (2017). Nanostructured mixed transition metal

oxides for high performance asymmetric supercapacitors: facile synthetic strategy. *Int. J. Hydrog. Energy* 42, 12384–12395. doi: 10.1016/j.ijhydene.2017.03.117

Trudeau, M. L. (2013). Advanced materials for energy storage. *MRS Bull.* 24, 23–26. doi: 10.1557/S0883769400053410

Wang, G. P., Zhang, L., and Zhang, J. J. (2012). A review of electrode materials for electrochemical supercapacitors. *Chem. Soc. Rev.* 41, 797–828. doi: 10.1039/C1CS15060J

Wang, H., Fu, Q., and Pan, C. (2019). Green mass synthesis of graphene oxide and its MnO$_2$ composite for high performance supercapacitor. *Electrochim. Acta* 312, 11–21. doi: 10.1016/j.electacta.2019.04.178

Wang, J. G., Kang, F., and Wei, B. (2015). Engineering of MnO$_2$-based nanocomposites for high-performance supercapacitors. *Prog. Mater. Sci.* 74, 51–124. doi: 10.1016/j.pmatsci.2015.04.003

Wang, J. G., Yang, Y., Huang, Z. H., and Kang, F. (2011). Coaxial carbon nanofibers/MnO$_2$ nanocomposites as freestanding electrodes for high-performance electrochemical capacitors. *Electrochim. Acta* 56, 9240–9247. doi: 10.1016/j.electacta.2011.07.140

Wang, J. G., Yang, Y., Huang, Z. H., and Kang, F. (2012). Synthesis and electrochemical performance of MnO$_2$/CNTs−embedded carbon nanofibers nanocomposites for supercapacitors. *Electrochim. Acta* 75, 213–219. doi: 10.1016/j.electacta.2012.04.088

Wang, J. G., Yang, Y., Huang, Z. H., and Kang, F. (2013). Effect of temperature on the pseudo-capacitive behavior of freestanding MnO$_2$@carbon nanofibers composites electrodes in mild electrolyte. *J. Power Sources* 224, 86–92. doi: 10.1016/j.jpowsour.2012.09.075

Wang, L., Huang, M., Chen, S., Kang, L., He, X., Lei, Z., et al. (2017). δ-MnO$_2$ nanofiber/single-walled carbon nanotube hybrid film for all-solid-state flexible supercapacitors with high performance. *J. Mater. Chem. A* 5, 19107–19115. doi: 10.1039/C7TA04712F

Wang, N., Wu, C., Li, J., Dong, G., and Guan, L. (2011). Binder-free manganese oxide/carbon nanomaterials thin film electrode for supercapacitors. *ACS Appl. Mater. Interfaces* 3, 4185–4189. doi: 10.1021/am201145k

Wang, T., Song, D., Zhao, H., Chen, J., Zhao, C., Chen, L., et al. (2015). Facilitated transport channels in carbon nanotube/carbon nanofiber hierarchical composites decorated with manganese dioxide for flexible supercapacitors. *J. Power Sources* 274, 709–717. doi: 10.1016/j.jpowsour.2014.10.102

Wang, X., Chen, L., Zhang, S., Chen, X., Li, Y., Liu, J., et al. (2019a). Compounding δ-MnO$_2$ with modified graphene nanosheets for highly stable asymmetric supercapacitors. *Colloid Surf.* 573, 57–66. doi: 10.1016/j.colsurfa.2019.04.040

Wang, X., Wu, D., Song, X., Du, W., Zhao, X., and Zhang, D. (2019b). Review on carbon/polyaniline hybrids: design and synthesis for supercapacitor. *Molecules* 24:2263. doi: 10.3390/molecules24122263

Wang, Y., and Igor, Z. (2009). Electrophoretic deposition of manganese dioxide-multiwalled carbon nanotube composites for electrochemical supercapacitors. *Langmuir* 25, 9684–9689. doi: 10.1021/la900937e

Wang, Y., Qu, Q., Gao, S., Tang, G., Liu, K., He, S., et al. (2019). Biomass derived carbon as binder-free electrode materials for supercapacitors. *Carbon* 155, 706–726. doi: 10.1016/j.carbon.2019.09.018

Wazir, A. H., and Kakakhel, L. (2009). Preparation and characterization of pitch-based carbon fibers. *N. Carbon Mater.* 24, 83–88. doi: 10.1016/S1872-5805(08)60039-6

Wei, H., Wang, X., Zhang, Y., Du, W., Sun, X., Jiang, F., et al. (2019). Facile synthesis of lotus seedpod-based 3D hollow porous activated carbon/manganese dioxide composite for supercapacitor electrode. *J. Electroanal. Chem.* 853:113561. doi: 10.1016/j.jelechem.2019.113561

Wei, L., Liu, J., and Zhao, D. (2016). Mesoporous materials for energy conversion and storage devices. *Nat. Rev. Mater.* 1:16023. doi: 10.1038/natrevmats.2016.23

Wei, W., Cui, X., Chen, W., and Ivey, D. G. (2011). Manganese oxide-based materials as electrochemical supercapacitor electrodes. *Chem. Soc. Rev.* 40, 1697–1721. doi: 10.1039/C0CS00127A

Wu, Z. S., Ren, W., Wang, D. W., Li, F., Liu, B., and Chen, H. M. (2010). High-energy MnO$_2$ nanowire/graphene and graphene asymmetric electrochemical capacitors. *ACS Nano* 4, 5835–5842. doi: 10.1021/nn101754k

Xiao, W., Xia, H., Fuh, J. Y. H., and Lu, L. (2010). Electrophoretic-deposited CNT/MnO$_2$ composites for high-power electrochemical

energy storage/conversion applications. *Phys. Scr.* 139:014008. doi: 10.1088/0031-8949/2010/T139/014008

Xie, S., Si, L., Cheng, F., and Lu, X. (2017). Recent advances for achieving high-performance carbon fiber materials for supercapacitors. *ChemElectroChem* 5, 571–582. doi: 10.1002/celc.201701020

Xie, X., Ni, C., Wang, B., Zhang, Y., Zhao, X., Liu, L., et al. (2019). Recent advances in hydrogen generation process via hydrolysis of Mg-based materials: a short review. *J. Alloys Compd.* 816:152634. doi: 10.1016/j.jallcom.2019.152634

Xie, Y., Yang, C., Chen, P., Yuan, D., and Guo, K. (2019). MnO$_2$-decorated hierarchical porous carbon composites for high-performance asymmetric supercapacitors. *J. Power Sources* 425, 1–9. doi: 10.1016/j.jpowsour.2019.03.122

Xin, L., and Wei, B. (2012). Facile synthesis and super capacitive behavior of SWNT/MnO$_2$ hybrid films. *Nano Energy* 1, 479–487. doi: 10.1016/j.nanoen.2012.02.011

Yan, J., Fan, Z., Wei, T., Cheng, J., Shao, B., Wang, K., et al. (2009). Carbon nanotube/MnO$_2$ composites synthesized by microwave-assisted method for supercapacitors with high power and energy densities. *J. Power Sources* 194, 1202–1207. doi: 10.1016/j.jpowsour.2009.06.006

Yan, J., Fan, Z., Wei, T., Qian, W., Zhang, M., and Wei, F. (2010). Fast and reversible surface redox reaction of graphene-MnO$_2$ composites as supercapacitor electrodes. *Carbon* 48, 3825–3833. doi: 10.1016/j.carbon.2010.06.047

Yang, Z., Zhang, J., Kintner-Meyer, M. C., Lu, X., Choi, D., Lemmon, J. P., et al. (2011). Electrochemical energy storage for green grid. *Chem. Rev.* 111, 3577–3613. doi: 10.1021/cr100290v

Yu, Z., Shang, J., Fu, W., Li, Z., and Cai, Y. (2018). A sp^2 + sp^3 hybridized carbon allotrope transformed from AB stacking graphyne and THD-graphene. *AIP Adv.* 8:015028. doi: 10.1063/1.5016387

Zhang, B., Kang, F., Tarascon, J. M., and Kim, J. K. (2015). Recent advances in electrospun carbon nanofibers and their application in electrochemical energy storage. *Prog. Mater. Sci.* 76, 319–380. doi: 10.1016/j.pmatsci.2015.08.002

Zhang, J., Sun, J., Shifa, T. A., Wang, D., Wu, X., and Cui, Y. (2019). Hierarchical MnO$_2$/activated carbon cloth electrode prepared by synchronized electrochemical activation and oxidation for flexible asymmetric supercapacitors. *Chem. Eng. J.* 372, 1047–1055. doi: 10.1016/j.cej.2019.04.202

Zhang, J., Wang, Y., Zang, J., Xin, G., Yuan, Y., and Qu, X. (2012). Electrophoretic deposition of MnO$_2$-coated carbon nanotubes on a graphite sheet as a flexible electrode for supercapacitors. *Carbon* 50, 5196–5202. doi: 10.1016/j.carbon.2012.07.002

Zhang, L. L., and Zhao, X. S. (2009). Carbon-based materials as supercapacitor electrodes. *Chem. Soc. Rev.* 38, 2520–2531. doi: 10.1039/b813846j

Zhang, Q., Wu, X., Zhang, Q., Yang, F., Dong, H., Sui, J., et al. (2019). One-step hydrothermal synthesis of MnO$_2$/graphene composite for electrochemical energy storage. *J. Electroanal. Chem.* 837, 108–115. doi: 10.1016/j.jelechem.2019.02.031

Zhang, Q. Z., Zhang, D., Miao, Z. C., Zhang, X. L., and Chou, S. L. (2018). Research progress in MnO$_2$-carbon based supercapacitor electrode materials. *Small* 14:1702883. doi: 10.1002/smll.201702883

Zhao, C., Ge, Z., Zhou, Y., Huang, Y., Wang, G., and Qian, X. (2017). Solar-assisting pyrolytically reclaimed carbon fiber and their hybrids of MnO$_2$/RCF for supercapacitor electrodes. *Carbon* 114, 230–241. doi: 10.1016/j.carbon.2016.12.025

Zhao, H., Han, W., Lan, W., Zhou, J., Zhang, Z., Fu, W., et al. (2016). Bubble Carbon-nanofibers decorated with MnO$_2$ nanosheets as high-performance supercapacitor electrode. *Electrochim. Acta* 222, 1931–1939. doi: 10.1016/j.electacta.2016.12.007

Zhi, M., Manivannan, A., Meng, F., and Wu, N. (2012). Highly conductive electrospun carbon nanofiber/MnO$_2$ coaxial nano-cables for high energy and power density supercapacitors. *J. Power Sources* 208, 345–353. doi: 10.1016/j.jpowsour.2012.02.048

Zhou, M., Gomez, J., Li, B., Jiang, Y. B., and Deng, S. (2017). Oil tea shell derived porous carbon with an extremely large specific surface area and modification with MnO$_2$ for high-performance supercapacitor electrodes. *Appl. Mater. Today* 7, 47–54. doi: 10.1016/j.apmt.2017.01.008

Zhu, G., He, Z., Chen, J., Zhao, J., Feng, X., Ma, Y., et al. (2014). Highly conductive three-dimensional MnO$_2$-carbon nanotube-graphene-Ni hybrid foam as a binder-free supercapacitor electrode. *Nanoscale* 6, 1079–1085. doi: 10.1039/C3NR04495E

Zhu, M., Wang, Z., Li, H., Yuan, X., and Zhi, C. (2018). Light-permeable, photoluminescent microbatteries embedded in the color filter of a screen. *Energy Environ. Sci.* 11, 2414–2422. doi: 10.1039/C8EE00590G

NOMENCLATURE

Acronyms	Full name
AC	Activated carbon
B-CNFs	Bubble carbon nanofibers
CA	Carbon aerogel
CFRP	Carbon fiber-reinforced polymer
CNFs	Carbon nanofibers
CNTs	Carbon nanotubes
CVD	Chemical vapor deposition
ECNF	Electrospun carbon nanofiber
EDLCs	Electrochemical double-layer capacitors
EDS	Energy-dispersive X-ray spectroscopy
EES	Electrochemical energy storage
GO	Graphene oxide
MnO_2	Manganese dioxide
MRCF	MnO_2/regenerated carbon fiber
MWCNTs	Multi-walled carbon nanotubes
PAN	Polyacrylonitrile
PEG	Polyethylene glycol
PVA	Polyvinyl alcohol
RCF	Regenerated carbon fiber
rGO	Reduced graphene oxide
SDS	Sodium dodecyl sulfate
SWCNTs	Single-walled carbon nanotubes
ZnO NPs	ZnO nanoparticles